Effect of Volcanic Eruptions on the Vertical Temperature Profile in Radiosonde Data and Climate Models

MELISSA FREE

NOAA/Air Resources Laboratory, Silver Spring, Maryland

JOHN LANZANTE

NOAA/Geophysical Fluid Dynamics Laboratory, Princeton, New Jersey

(Manuscript received 7 April 2008, in final form 4 December 2008)

ABSTRACT

Both observed and modeled upper-air temperature profiles show the tropospheric cooling and tropical stratospheric warming effects from the three major volcanic eruptions since 1960. Detailed comparisons of vertical profiles of Radiosonde Atmospheric Temperature Products for Assessing Climate (RATPAC) and Hadley Centre Atmospheric Temperatures, version 2 (HadAT2), radiosonde temperatures with output from six coupled GCMs show good overall agreement on the responses to the 1991 Mount Pinatubo and 1982 El Chichón eruptions in the troposphere and stratosphere, with a tendency of the models to underestimate the upper-tropospheric cooling and overestimate the stratospheric warming relative to observations. The cooling effect at the surface in the tropics is amplified with altitude in the troposphere in both observations and models, but this amplification is greater for the observations than for the models. Models and observations show a large disagreement around 100 mb for Mount Pinatubo in the tropics, where observations show essentially no change, while models show significant warming of ~0.7 to ~2.6 K. This difference occurs even in models that accurately simulate stratospheric warming at 50 mb. Overall, the Parallel Climate Model is an outlier in that it simulates more volcanic-induced stratospheric warming than both the other models and the observations in most cases.

From 1979 to 1999 in the tropics, RATPAC shows a trend of less than 0.1 K decade^{-1} at and above 300 mb before volcanic effects are removed, while the mean of the models used here has a trend of more than 0.3 K decade^{-1}, giving a difference of ~0.2 K decade^{-1}. At 300 mb, from 0.02 to 0.10 K decade^{-1} of this difference may be due to the influence of volcanic eruptions, with the smaller estimate appearing more likely than the larger. No more than ~0.03 K of the ~0.1-K difference in trends between the surface and troposphere at 700 mb or below in the radiosonde data appears to be due to volcanic effects.

1. Introduction

Changes in the vertical temperature profile, which may be useful for climate change assessment and detection and attribution studies, can be affected by volcanic eruptions. The lack of long-term warming in the tropical troposphere relative to the surface in some radiosonde observations is not yet fully explained (Karl et al. 2006), and the possible role of volcanic eruptions in this trend difference has not been fully explored. The World Climate Research Programme's (WCRP's) Coupled Model Intercomparison Project, phase 3 (CMIP3; Meehl et al. 2007), twentieth-century coupled climate model experiments provide an opportunity to compare the observed volcanic effects to those seen in the models and to examine possible effects of the eruptions on vertical temperature trend profiles.

Volcanic effects on observed stratospheric and surface temperatures have been examined previously in many papers (see Angell 1997a; Robock 2000, and references therein). A basic problem in studying volcanic effects is the fact that eruptions often coincide with ENSO events, which can obscure the effects of the volcanic aerosols. In the stratosphere, the quasi-biennial oscillation (QBO) similarly tends to complicate the identification of volcanic signals. Some studies show cooling in the troposphere following the 1991 eruption of Mount

Corresponding author address: Melissa Free, 1315 East-West Highway, NOAA/Air Resources Laboratory, Silver Spring, MD 20910.
E-mail: melissa.free@noaa.gov

DOI: 10.1175/2008JCLI2562.1

Pinatubo, but the tropospheric effects of El Chichón in 1982 were less clear because of the influence of the large ENSO at that time (Parker 1985; Parker et al. 1996; Angell 1988). Stenchikov et al. (2004), Ramachandran et al. (2000), and others compared observed and modeled temperature responses to Mount Pinatubo with emphasis on the winter warming effect at the surface in the northern extratropics, and Stenchikov et al. (2006) used the CMIP3 model archive to study the winter warming effect for a larger number of eruptions in the twentieth century. Santer et al. (2001) showed that volcanoes and ENSO could affect differential temperature trends in Microwave Sounding Unit (MSU) lower-tropospheric temperature (TLT) and surface data, but that the extent of that effect was difficult to determine. Most of these studies looked at either layer mean temperatures or those at individual atmospheric levels rather than detailed vertical temperature profiles.

Lanzante (2007) conducted a limited examination of volcanic signals in a version of the Geophysical Fluid Dynamics Laboratory (GFDL) general circulation model (GCM) that preceded the current model and concluded that errors in those signals might have a significant effect on modeled tropospheric trends. On the other hand, trend profiles for 1979–99 for model runs without volcanic forcing do not appear to differ systematically from runs with volcanoes (Santer et al. 2005). This may mean either that the true volcanic effect on trends is negligible for this time period or that the true effects are significant but are not reproduced properly by the models. Free and Angell (2002) showed the profiles of volcanic temperature effects in an earlier radiosonde dataset. Here we use two new radiosonde datasets in comparison with selected CMIP3 twentieth-century climate model outputs to see how well the volcanic signal is reproduced by the models, and we attempt to estimate its potential effect on trends in the troposphere and lower stratosphere, with particular emphasis on the tropical troposphere.

2. Data and methods

We use radiosonde data from the Radiosonde Atmospheric Temperature Products for Assessing Climate (RATPAC; Free et al. 2005) and Hadley Centre Atmospheric Temperatures, version 2 (HadAT2; Thorne et al. 2005), datasets, which have been adjusted to reduce inhomogeneities resulting from changes in instruments and measurement practices. RATPAC includes 85 stations located throughout the globe, and HadAT2, a gridded product, is derived from data at 676 stations. RATPAC data exist for 13 atmospheric levels, while HadAT2 has 9 levels. The two datasets use different homogeneity adjustment methods. Because most results are very similar for RATPAC and HadAT2, we show only RATPAC in the figures below (except for Fig. 4).

We define the volcanic signal as the mean of temperatures for the 2 yr after the eruption minus the mean temperature for 2 yr before the eruption. We use 2 yr before the eruption as a base period to average out some of the natural variability while minimizing the effect of long-term trends. Stenchikov et al. (2006) used a longer base period (~6 yr for El Chichón and Mount Pinatubo) and Lanzante (2007) used 2–4 yr, while Santer et al. (2001) used just 4–12 months before the eruption. We get similar results whether we use 2 or 5 yr before the eruption. Using shorter or longer intervals instead of 24 months after the eruption has a greater effect, but does not change our conclusions.

Before computing the volcanic signal in the observations we estimate and remove the effects of ENSO and the QBO based on linear regression using the surface temperature in the Niño-3.4 area (Niño-3.4) or the Southern Oscillation index (SOI) and the 50-mb Singapore winds, respectively (Free and Angell 2002). As an alternative we also used an iterative method similar to that of Santer et al. (2001) to separate the volcanic and ENSO signals and tested several alternative QBO removal approaches (see below).

We compare the resulting signals in observations to those calculated from the output of twentieth-century simulations for six coupled climate models in the CMIP3 archive that include volcanic forcing, which varies between the six models as shown in Table 1. These same models, as well as both radiosonde datasets, were used recently to examine the vertical structure of temperature trends in the troposphere and lower stratosphere (Lanzante and Free 2008). The runs also include anthropogenic and solar forcings. In computing the volcanic signals in the models we do not remove QBO effects because few if any coupled GCMs show significant QBO signals (Randall et al. 2007). We subsample the model grid to use only those grid boxes containing radiosonde stations in the RATPAC or HadAT2 networks and remove estimated ENSO effects calculated in the same way as for the observations. Uncertainty of the observed signals is determined by a Student's t test, while the significance of the difference between the observed and modeled signals is assessed using a paired-sample t test.

Accounting for QBO and ENSO effects

One way to remove the confounding effects of the QBO and ENSO on our assessments of volcanic signals is based on stepwise regression, by first removing the QBO signal and then the ENSO signal. We regress

TABLE 1. Models used, with source for volcanic forcing, number of realizations of the twentieth-century experiment, and reference for the model. The GISS model runs used here are revised runs using corrected ozone forcings.

Modeling center	Model	No. of runs	Volcanic forcing	Reference
Geophysical Fluid Dynamics Laboratory	CM2.0	3	Sato et al. (1993) and Ramachandran et al. (2000)	Delworth et al. (2006)
Geophysical Fluid Dynamics Laboratory	Climate Model, version 2.1 (CM2.1)	3	Sato et al. (1993) and Ramachandran et al. (2000)	Delworth et al. (2006)
Goddard Institute for Space Studies	GISS-ER (revised runs)	5	Sato et al. (1993)	Hansen et al. (2007)
Goddard Institute for Space Studies	GISS Model E-H (GISS-EH) EH (revised runs)	5	Sato et al. (1993)	Hansen et al. (2007)
Hadley Centre, Met Office	HadGEM	1	Sato et al. (1993)	Johns et al. (2006)
NCAR	PCM	4	Ammann et al. (2003)	Washington et al. (2000)

observed temperatures on the QBO index, subtract the resulting QBO signal from the temperatures, and then regress the resulting residual against an ENSO index. Although the residual signals after the QBO regression signal is subtracted are not correlated with the QBO indices, it is possible that some nonlinear QBO effect could remain in the time series. However, when the time series are averaged over 24 months, any such signal will be very small. The volcanic signals produced using two alternative QBO regression methods (either using the difference between 30- and 50-mb Singapore winds, or regressing ENSO and QBO indices simultaneously using singular value decomposition) are very similar to those shown below. The alternative QBO signals (not shown) differ by no more than 0.2 K when averaged over the 24 months after the eruptions.

We also used several approaches to separate the ENSO and volcanic signals, including linear regression and the iterative method described in Santer et al. (2001), to assess the sensitivity of our results to ENSO removal methods. The indices and temperature series were detrended prior to the regression, and the 3 yr after each of the three major volcanic eruptions were excluded in order to reduce the colinearity problems described in Santer et al. (2001).

The method of Santer et al. (2001) involves an iterative procedure alternating between the removal of ENSO and the volcanic signals from a time series. The procedure assumes that the volcanic signal takes the form of a linear ramp-down to a peak cooling, followed by exponential decay with a specified decay constant. Figure 1 shows an example of this assumed volcanic signal. Additional details are given in the appendix.

We repeated linear regression calculations for the RATPAC observations using either the SOI or Niño-3.4 indices, and for the time periods of 1958–99, 1958–77, and 1977–99 to test the stability of the regression relation over time. The ENSO indices were lagged by 4 months. Figure 2 shows the mean of these ENSO signals for the region from 30°N to 30°S averaged over the 2 yr after Mount Pinatubo for some of these methods, along with results for the troposphere from the iterative procedure as described in Santer et al. (2001; for levels up to 150 mb only).

The ENSO signal estimates range from ~0.3 to ~0.5 K in the upper troposphere. While SOI yields more tropospheric warming than SST, and the iterative method yields more than the noniterative, the choice of index (SOI versus SST) has a larger impact than the method (iterative versus noniterative). The regression coefficients are similar for the different time periods tested. The signal in the tropical stratosphere is comparable in size to that in the troposphere, as found in Lau et al. (1998). Because the tropospheric signal is similar in size to the observed volcanic effects, our assessment of the size of the volcanic signal will depend on the choice of ENSO signal estimation method.

For the model output we use modeled surface air temperature in the Niño-3.4 area for the ENSO regression. We tested SSTs from other tropical Pacific areas using the GFDL model and found that Niño-3.4 was at least as well correlated with tropical tropospheric temperatures as were the alternatives. For the Goddard Institute for Space Studies Model E-R (GISS-ER), which has little ENSO variability, the SST signal was dominated

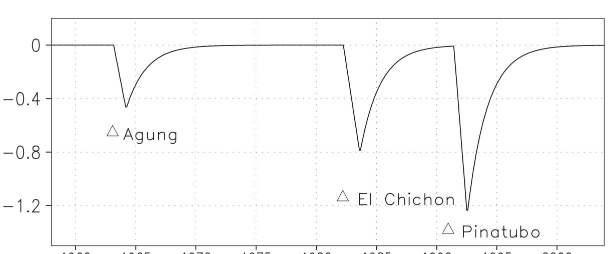

FIG. 1. Example of form of volcanic temperature signal assumed in the iterative method for the troposphere. Triangles show times of the three major eruptions.

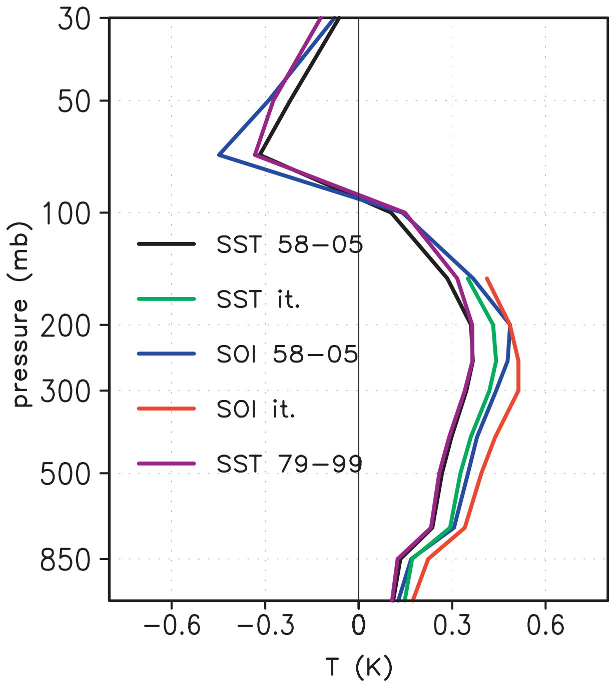

FIG. 2. Mean over the 2 yr after Mount Pinatubo of the ENSO temperature signal (K) in RATPAC observations for the tropics (30°N–30°S) derived by a single linear least squares regression using Niño-3.4 SSTs for 1958–2005 (SST 58–05) and for 1979–99 (SST 79–99), the Southern Oscillation index for 1958–2005 (SOI 58–05), and by an iterative procedure as in Santer et al. (2001) using SSTs (SST it.) and the SOI (SOI it.).

by volcanic cooling rather than ENSO-like changes. For that model, our "ENSO removal" may actually remove a significant part of the volcanic signal, and results for GISS-ER may be understated for that reason.

Because the iterative procedure is not applicable without modification in the stratosphere or around the tropopause, and because of uncertainties arising in the application of this method to noisy data, we rely more heavily on the signal derived from noniterative linear regression.

3. Volcanic signal using noniterative method

Figure 3 shows the latitude–altitude distribution of the effects of Mount Agung, El Chichón, and Mount Pinatubo in the RATPAC observations and the mean of all six model responses. While all show the expected tropospheric cooling and stratospheric warming, the model mean generally shows more stratospheric warming and less upper-tropospheric cooling in the tropics than in the observations. The observations show a stratospheric warming at high southern latitudes after Mount Pinatubo that is not seen in the models. This warming could be due to the eruption of Cerro Hudson at 46°S in August 1991 (Deshler et al. 1992), although it could also reflect errors in the observed signal resulting from the small number of stations present at those latitudes. For Mount Agung, the models show much more cooling in the tropics and NH than is seen in the observations, but the observations are less reliable during this earlier time period.

We next examine the profiles of these effects in more detail in three latitude regions: the tropics (30°S–30°N), NH extratropics (30°–90°N), and SH extratropics (90°–30°S), showing results for individual model ensemble means.

a. Tropics

Figure 4 shows the volcanic signal for each latitude zone using RATPAC and HadAT2 and the ensemble means for each of the six models. In the tropical troposphere, the observations and the majority of the models show tropospheric amplification of surface cooling for Mount Pinatubo and El Chichón. The exceptions are GISS-ER, which has little cooling anywhere for either Mount Pinatubo or El Chichón, and the Hadley Centre Global Environmental Model (HadGEM), which has little cooling for El Chichón. Most models show the ratio of El Chichón cooling to Mount Pinatubo cooling in the tropical troposphere to be around 0.3–0.6, but these observations show El Chichón to be much more similar to Mount Pinatubo in the lower troposphere and at 50 mb, a result that is inconsistent with expectations. Based on the generally accepted relationship between the aerosol loadings for the two eruptions (Sato et al. 1993; McCormick et al. 1995), and with results from Santer et al. (2001) using global MSU and surface temperature records, we would expect the El Chichón effect to be no more than 2/3 that of Mount Pinatubo.

In the tropical stratosphere, the Parallel Climate Model (PCM) and HadGEM responses to Mount Pinatubo are much larger than those of RATPAC, GISS-ER responses are slightly larger, and GFDL Climate Model version 2.0 (CM2.0) is slightly smaller. The greatest model–observation difference is at 100 mb for Mount Pinatubo where all models show significantly more warming than the observations. This is not simply a function of excessive modeled warming in the stratosphere, because the GFDL model results are close to observations at 50 and 70 mb, and yet show warming of ~0.7 K at 100 mb where the observations show no change. For El Chichón, the GFDL CM2.0 and GISS-ER responses are smaller than the observations in the stratosphere, while PCM and HadGEM are larger by almost 1 K. At 100 mb, observations for El Chichón show

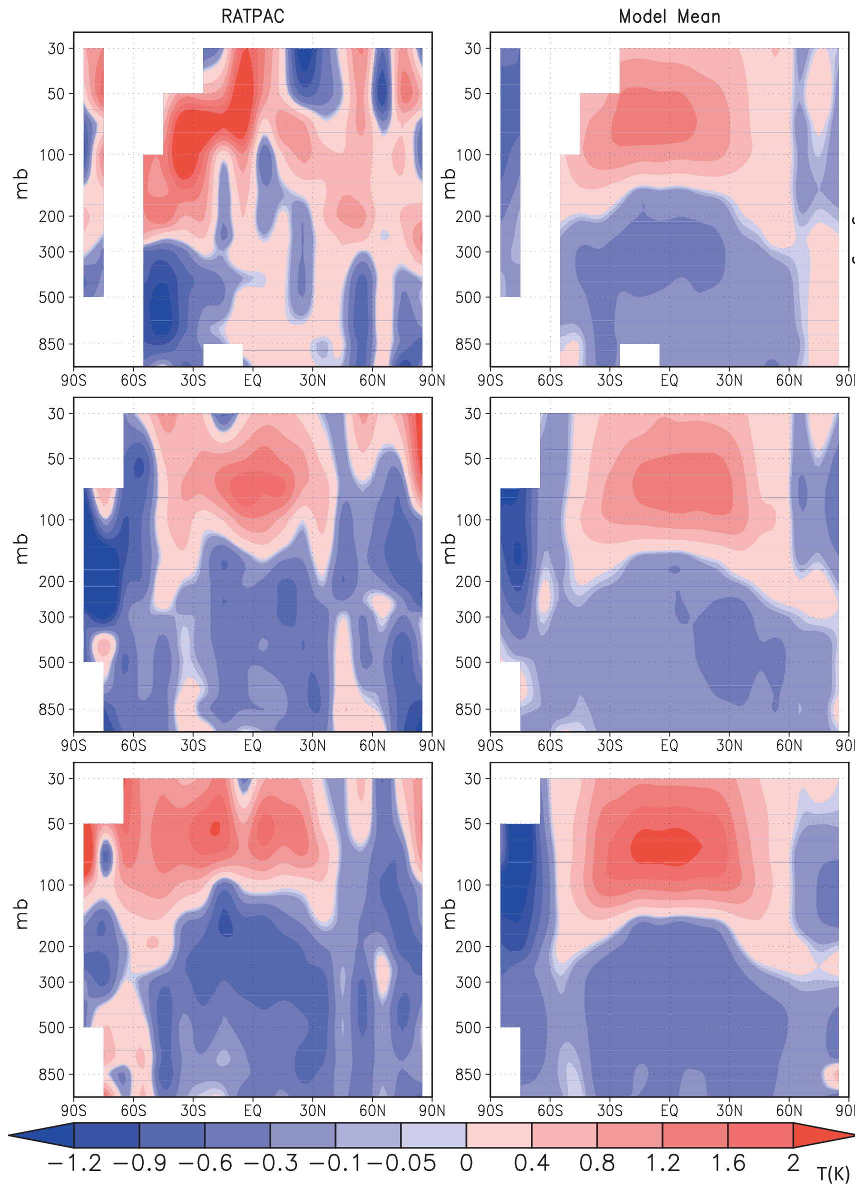

FIG. 3. Mean change in temperature after the volcanic eruptions of (top) Mount Agung, (middle) El Chichón, and (bottom) Mount Pinatubo in (left) RATPAC observations and (right) the mean of models, as measured by the mean temperature for 2 yr after the eruption minus the mean for 2 yr before.

warming, and four of the six models give reasonably similar results, but those four models give insufficient warming at 70 mb. HadAT2 gives similar results to RATPAC in the tropics except for Mount Agung. Because HadAT2 does not include data at 70 mb, the location of the maximum stratospheric warming is not as clear in that dataset.

Figures 5a,b are time series of model ensemble means and RATPAC data at 50 and 100 mb in the tropics for 1988 to 1997. At 50 mb, the modeled and observed temperatures are fairly close to each other for the first year after Mount Pinatubo and then the observations drop much more than the models. It appears that much of the difference between observed and simulated 24-month mean signals at this level comes from the second year rather than the first. At 100 mb, the models show clear warming signals in the first post–Mount Pinatubo year, but the data show no consistent warming, confirming the difference seen in the 24-month mean signal plots. At this level, the model-observed difference arises primarily in the first year rather than the second year after the eruption.

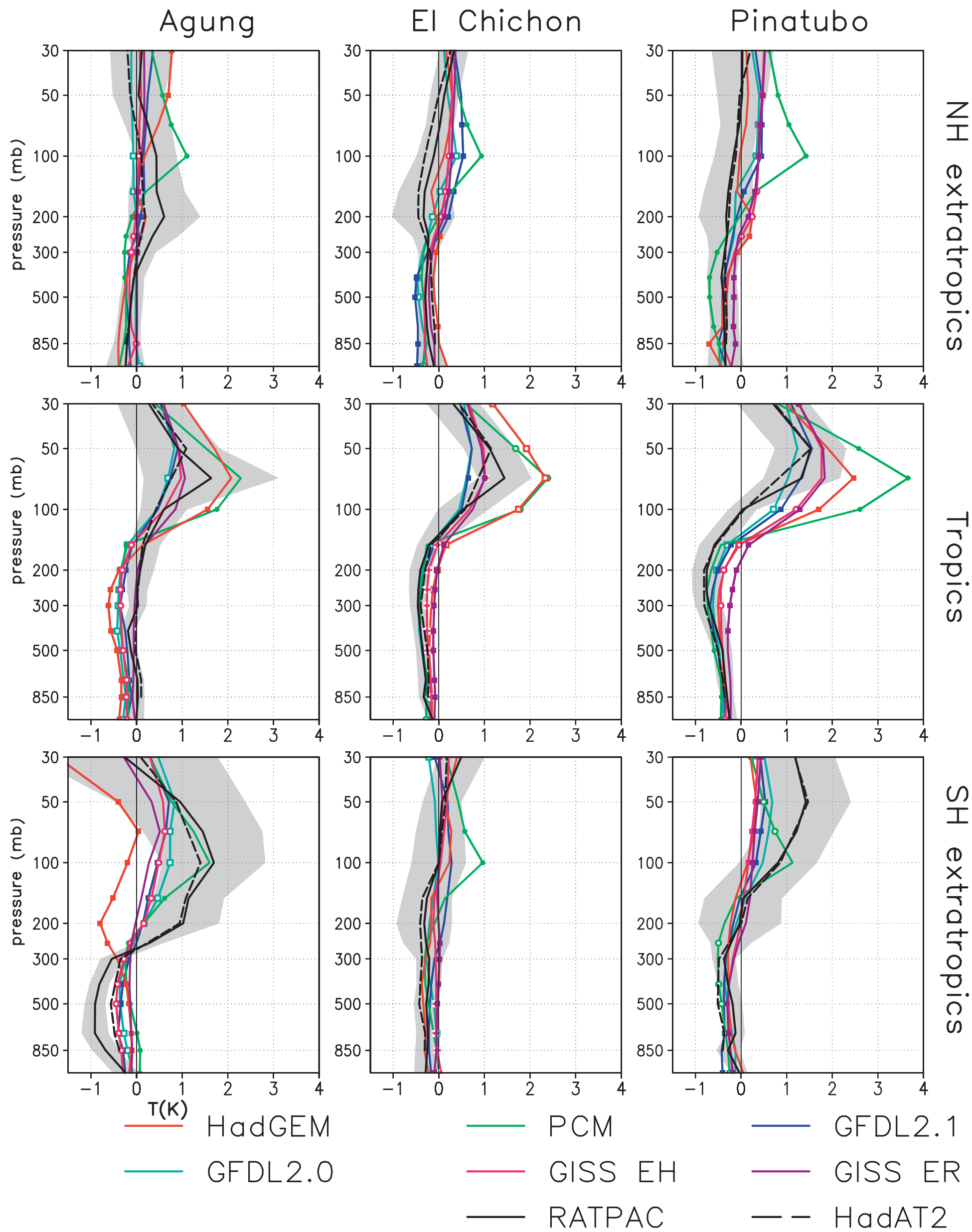

FIG. 4. Responses to volcanic eruptions in RATPAC and HadAT2 data and model ensemble means for (top) Northern Hemisphere extratropics, (middle) tropics, and (bottom) Southern Hemisphere extratropics: mean temperature (K) for the 2 yr after each eruption minus mean temperature for 2 yr before, after subtracting the ENSO and QBO effects. Gray area is the 95% confidence interval for the RATPAC observations. Symbols denote model responses that are significantly different from the RATPAC responses. Model output has been subsampled according to the RATPAC station locations.

b. NH extratropics

In the NH extratropics (NHX) the RATPAC data for Mount Pinatubo show only small surface and tropospheric cooling and little or no stratospheric warming above 100 mb (Fig. 4). The model results are similar for the surface and lower troposphere, but most show warming from 200 to 100 mb in contrast to the observed cooling. PCM shows a warming of ~1.5 K peaking at 100 mb where the observations and other models show changes of −0.1 to +0.4 K. The vertical patterns for El Chichón generally resemble those for Mount Pinatubo, with PCM again showing a large warming at 100 mb that is not seen in the observations or other models.

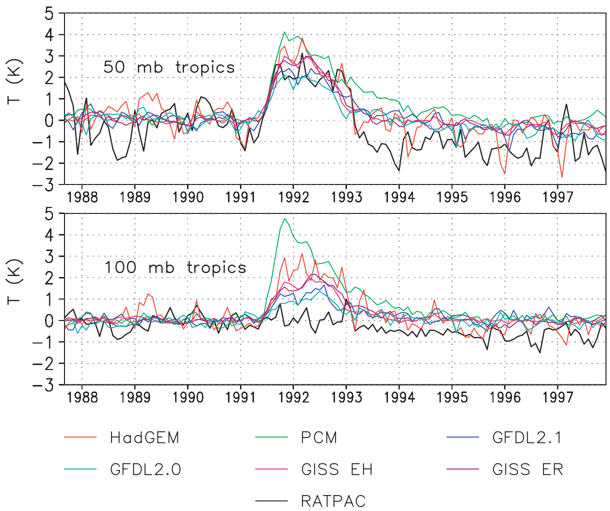

FIG. 5. Time series of temperatures at (top) 50 and (bottom) 100 mb in the tropics from RATPAC observations after subtracting QBO and ENSO signals, and from models after subtracting ENSO signals.

c. SH extratropics

Both Mount Pinatubo and El Chichón show small tropospheric coolings that are approximately uniform vertically in the SH extratropical (SHX) troposphere in observations and in most models. It is difficult to see much difference between the NHX and SHX in the amount of cooling after these two eruptions. Mount Agung shows a larger observed tropospheric cooling than either Mount Pinatubo or El Chichón in the SHX, despite a similar surface cooling. However, the observed cooling of almost 1 K in RATPAC is almost twice as large as that in HadAT2, so the statistically significant difference between models and RATPAC observations for Mount Agung does not appear to be robust.

In the SHX stratosphere, Mount Pinatubo and Mount Agung produced warmings of similar size in both RATPAC and HadAT2. Most of the models have less than 0.5-K stratospheric warming for Mount Pinatubo, which is much less than the observed 1.5 K. In contrast, El Chichón produced little or no stratospheric warming in either RATPAC or HadAT2, and the models simulate a similar lack of stratospheric warming (except for PCM). It should be kept in mind that the very limited spatial sampling of observations in the SH extratropics may play a major role in any apparent discrepancies between the models and observations there.

4. Results from the iterative method

Applying the iterative method of Santer et al. (2001; see the appendix for details) to the observations and models gives an alternative view of the volcanic signal. We use this method only in the troposphere because it depends on assumptions about the shape of the volcanic response that may not apply directly to the stratosphere. The observed volcanic signals estimated this way differ from those shown above mainly in the larger size of some signals, especially in the extratropics (Fig. 6). The observed tropical tropospheric response to Mount Agung is also much larger using this approach than in the analysis in the previous section. This may be due to a tendency of the iterative method to overstate the response in the presence of large internal variability, especially when the true signal is small (see the appendix). Model mean responses are similar in the tropics for both methods, but the iterative method again gives larger responses than the noniterative method for the extratropics (Fig. 7). Figure 7 also includes the model mean response without any ENSO removal, showing that the net ENSO effect after Mount Pinatubo is a tropical cooling in the models, in contrast to the warming effect in the observations. This is due to a large La Niña effect in the GFDL models.

5. Tropospheric amplification of surface changes

Most modeled and observed results show greater cooling aloft than at the surface in the tropics for both El Chichón and Mount Pinatubo. Figure 8 (left) shows the ratio of the tropospheric volcanic effect to the surface effect for Mount Pinatubo in the models and data using the noniterative approach for ENSO signal removal along with the result from the iterative effect for the observations. The observations show noticeably more amplification than the models for both Mount Pinatubo and El Chichón (not shown). For both eruptions, the results are generally similar if the iterative method is used, except that for Mount Pinatubo, HadGEM shows amplification similar to that of the observations. Interestingly, the observations show a similar amplification for ENSO (Fig. 8, right) as for Pinatubo, but the models show stronger amplification for ENSO than for Mount Pinatubo, so that models and observations are in closer agreement on the ENSO response ratio than for the volcanic response. For most models this difference occurs even if we consider negative and positive SST events separately.

6. Effect on trends

a. Iterative method

Using the approach of Santer et al. (2001) gives an estimate of the size and shape of the cooling after the three eruptions. Using this, we estimate the effect of the

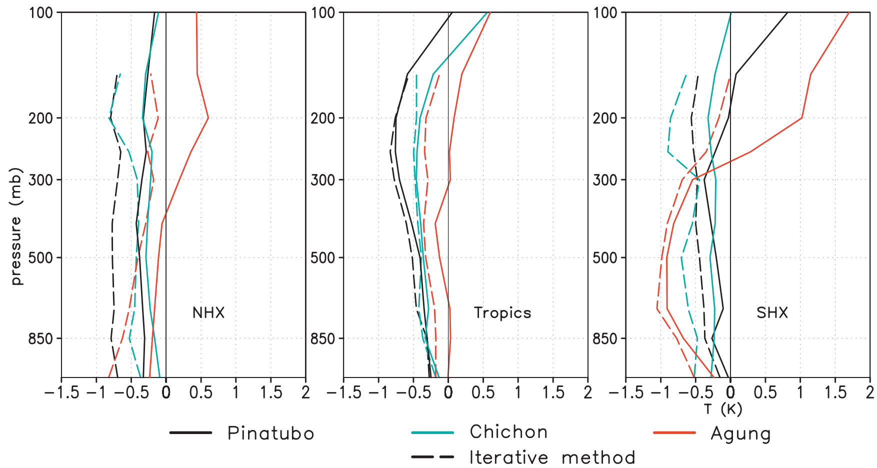

FIG. 6. Volcanic temperature signals (K) from noniterative (solid lines) and iterative (dashed lines) methods for the three eruptions in the RATPAC observations for the NH extratropics, SH extratropics, and tropics.

eruptions on tropospheric trends calculated by both the linear least squares regression (LS) and median of pairwise slopes (MPS; Lanzante 1996) methods by subtracting trends in the residual time series (after removal of the volcanic signal) from trends in the full time series. Although MPS has advantages over LS, LS is still often used in analysis of tropospheric trends, and some results differ noticeably between the two methods. Because the discrepancy between the observed and modeled trend profiles is greatest in the tropics (Lanzante and Free 2008), this discussion is limited to that region, and trend periods end in 1999 because most CMIP3 model experiments end then.

Trend effect results from the iterative method depend on the choice of the decay parameter and, to a lesser degree, the extent to which the data are smoothed before application of the method. Figure 9 shows results for the tropics using RATPAC observations, the mean of all six models, and a range of these parameter and smoothing choices. As one might expect from Fig. 8, in many cases the observations show greater trend effects in the upper troposphere than at the surface, suggesting possible volcanic effects on differential temperature trends. The model mean typically shows less differential effect than the observations. However, the trend effects are much larger for larger decay parameters than for smaller parameters, and only for decay parameters greater than 15 months is the effect larger than ~0.05 K decade^{-1}. For the observations, the effects are larger for MPS trends than for LS. Although the trend effects in most cases are net cooling, in some cases, for the smaller settings of the decay parameter, the apparent effect of

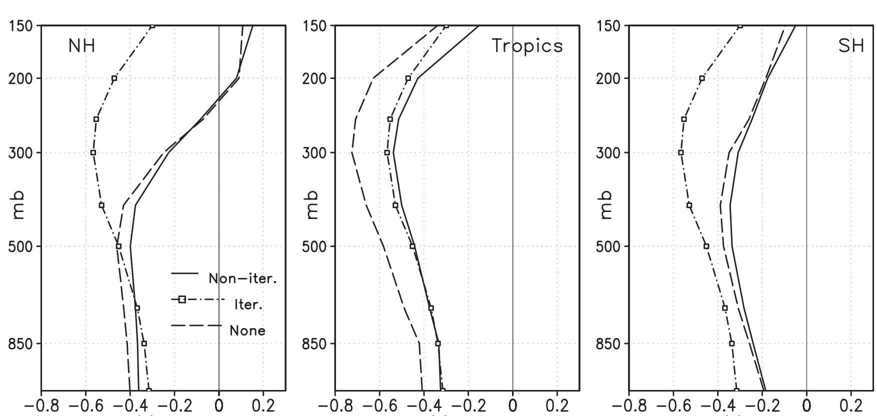

FIG. 7. Mean of Mount Pinatubo temperature response (K) for six model ensemble means from noniterative (non-iter) and iterative methods and without any ENSO removal procedure (none).

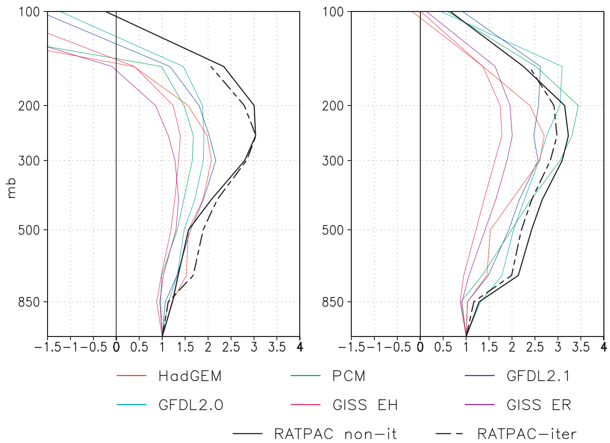

FIG. 8. (left) Temperature response to Mount Pinatubo in the troposphere divided by response at the surface for the tropics using noniterative ENSO removal for the models and RATPAC, and using iterative removal for RATPAC (RATPAC-iter.). (right) Tropospheric ENSO signal from noniterative linear regression divided by the signal at the surface, for the tropics, and for RATPAC observations using the iterative method (RATPAC-iter.) with a decay parameter of 20 months.

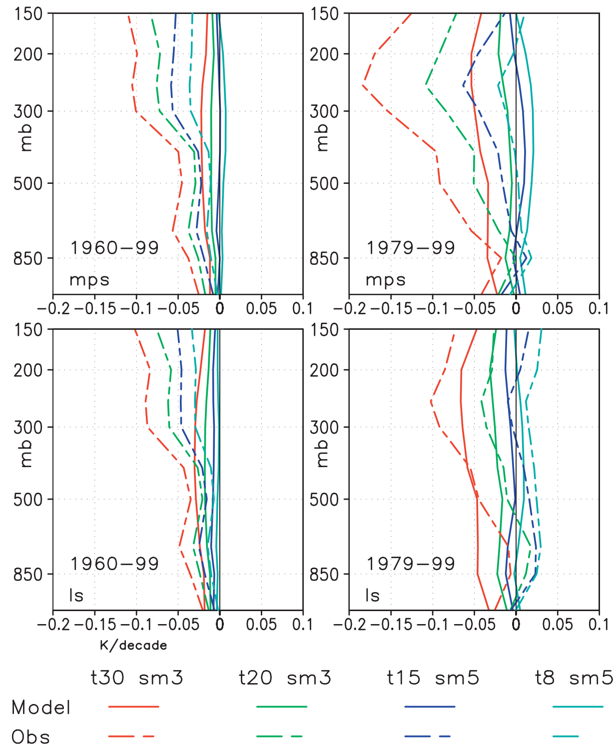

FIG. 9. Effects of volcanic eruptions on (top) median of pairwise slopes and (bottom) least squares temperature trends (K decade^{-1}) in RATPAC observations (obs) and the mean of six models (Model) for the tropics, derived using the iterative method of Santer et al. (2001), for (left) 1960–99 and (right) 1979–99, for decay parameters of 30 (t30), 20 (t20), 15 (t15), and 8 (t8) months, and for smoothing using 3- (sm3) and 5-month (sm5) running means. The quantity plotted is the difference in trend estimates from the raw time series minus those from the time series with volcanic effects removed.

the volcanic eruptions is a net warming trend. The trend effects for individual model ensemble means (Fig. 10) vary, but in all cases are less than those in the observations for the upper troposphere. Figure 11 (left) shows MPS trends after removing volcanic signals in the tropical troposphere for 1979–99 using a decay parameter of 30 months. This figure suggests that without the eruptions, MPS trends for RATPAC at 300 mb would have been similar to those from several models. However, this is not true for the least squares trends or for smaller choices of the decay parameter (Fig. 11, middle and right), which appear to fit the time series better (see the appendix). Only decay parameters of 20 months or greater give observed trends larger at 300 mb than at the surface; the sharp decrease in the observed trend from the surface to 850 mb remains in all cases.

The greater negative effect of volcanic responses on trends in the upper troposphere versus the surface in the observations than in the models could contribute up to 0.08 K decade^{-1} (at 300 mb) to the relative lack of amplification of surface trends in the upper troposphere for this time period using MPS (see Santer et al. 2005; Lanzante and Free 2008), but only if the decay time for the volcanic cooling is relatively long. This effect is less clear below 400 mb for any parameter setting and is much less for least squares trends than for MPS. At 700 mb and below, the differential effects of volcanoes on surface–troposphere trend differences for 1979–99 appear to be no more than ~0.03 K. For periods ending much after 1999, volcanic effects on trends would be expected to be even smaller.

b. *Dropping postvolcanic years*

An alternative way to estimate volcanic effects on trends that has been used in the past is to remove several years of data after the date of the eruptions and recalculate the trends using the shorter record. This method is likely to miss some of the trend effects to the extent that the cooling extends beyond the time period omitted. It also removes not just the volcanic effects but any other natural variations (such as ENSO) occurring during those years. We tested this method on the observations and model output and found that the estimated effects on trends depended on the length of the period of data removed. This dependence is less if ENSO and QBO signals are removed before trend calculations. Figure 12 shows the MPS trend resulting from volcanic effects, that is, the trend using all years minus the trend with two or four postvolcanic years removed, for the tropics, when ENSO and QBO are removed from all time series. For 1960–99 the effect of

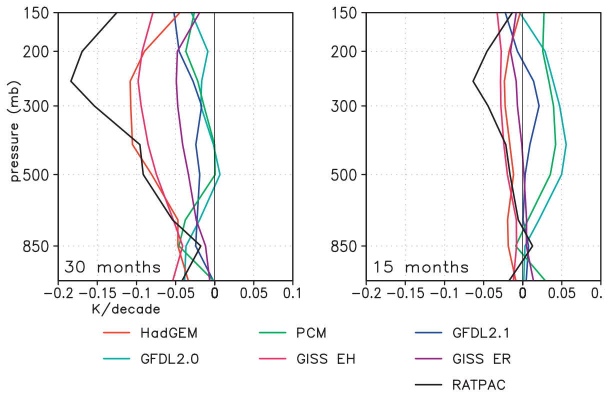

FIG. 10. Effects of volcanic eruptions on median of pairwise slope temperature trends (K $decade^{-1}$) in RATPAC observations and the six models for the tropics, derived using the iterative method of Santer et al. (2001) using decay parameter of (left) 30 months with 3-month smoothing and (right) 15 months with 5-month smoothing.

including the postvolcanic periods is to reduce the tropospheric trend in both models and observations, while for 1979–99 the predominant effect is small tropospheric warming. The differences between trend effects in the models and observations are generally less than 0.03 K $decade^{-1}$ for 1979–99 in the troposphere, or ~10% of the mean trend in the models, with little differential effect between the surface and the troposphere. Results using the least squares trends (not shown) are generally similar to those from MPS, except for models in the stratosphere. As might be expected, the results from this analysis resemble generally those from the iterative method if small values of the decay parameter are used.

7. Discussion

All models used here capture the basic pattern of tropospheric cooling and stratospheric warming in response to volcanic eruptions, but several models overstate the stratospheric warming, and all models disagree with observations at 100 mb for Mount Pinatubo. Because the models did not all use the same forcing data, and documentation about those forcings is not always complete, it is difficult to assign causes for the differences between the modeled and observed signals or between the model responses.

Although we did not test the statistical significance of differences between PCM and other models, the PCM responses are distinct enough from those of other models to require further discussion. The most important potential causes are the volcanic aerosol forcing inputs. All the models except PCM used forcing based on Sato et al. (1993). This dataset uses an aerosol effective radius that varies in space and time, and so is probably more realistic than the uniform radius in the forcing used by PCM. The latitudinal and vertical distribution of the aerosols also differs between the two datasets. This difference is the most likely reason for the outlier status of the PCM response in the stratosphere. PCM does not differ from the other models as a group in terms of vertical resolution or climate sensitivity, and we are not aware of any other likely explanation for the differences between the PCM volcanic response and that of the other models. The larger response by HadGEM could be the result of greater internal variability because HadGEM has only one realization rather than the three to five realizations that exist for the other models.

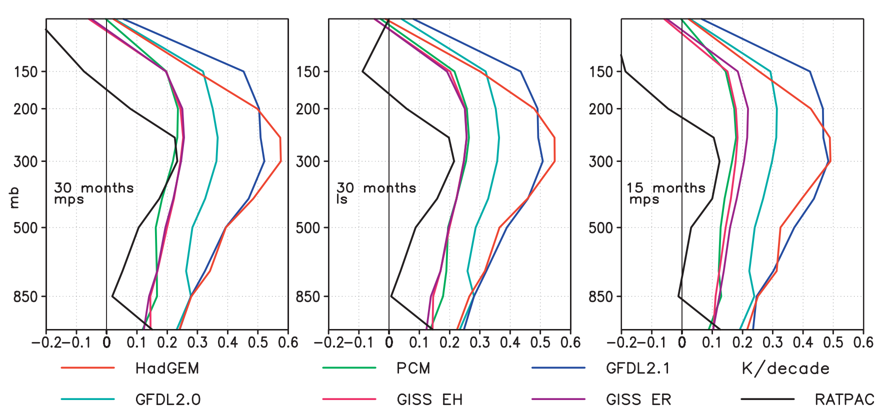

FIG. 11. Temperature trends after removing volcanic signals: median of pairwise slope trends for 1979–99 (K $decade^{-1}$) in the tropics in observed and modeled time series after subtracting the time series of the volcanic signal obtained using the iterative method of Santer et al. (2001), with a decay parameter of (left) 30 and (right) 15 months, and (middle) for least squares trends with decay parameter of 30 months.

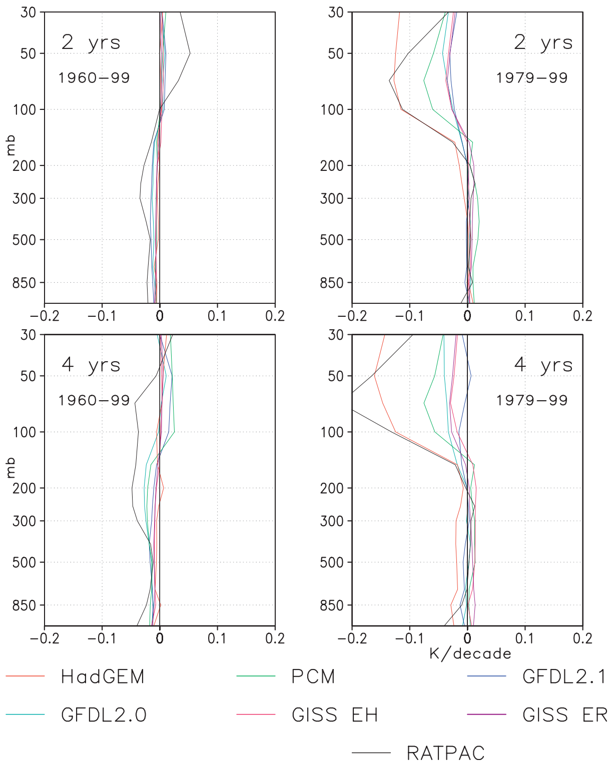

FIG. 12. Trends solely due to volcanic effects: median of pairwise slope trends (K $decade^{-1}$) for the tropics from full time series minus trends in series with (top) 2 or (bottom) 4 yr removed immediately after the three volcanic eruptions, for (left) 1960–99 and (right) 1979–99. ENSO signals have been removed before all trend calculations and QBO signals have been removed for the observations.

The difference between the models as a group and the observations in the 150–70-mb tropical layer after Mount Pinatubo is harder to explain. Because four of the six models do reasonably well in this layer for El Chichón, it seems unlikely that the difference is due to basic deficiencies in the models themselves. The models with the highest vertical resolution (HadGEM) or the highest model tops (GISS models) do not appear to give a better result in this respect than the others. A lack of significant warming at the tropopause is seen in the reanalysis data (Randel et al. 2000) after Mount Pinatubo, so the difference is probably not due to problems with the observations. Again, the most likely explanation would seem to be shortcomings in the forcing input.

Although the volcanic aerosol forcing near the tropopause could be wrong, the problem could also be inadequate specification of ozone or water vapor changes after Mount Pinatubo in this area. The simulations include the long-term downward trends in stratospheric ozone, but the documentation indicates that they do not include the short-term declines after recent volcanic eruptions. Whether these declines were sufficient in the tropics to account for the lack of warming after Mount Pinatubo around 100 mb is not clear. Stenchikov et al. (2004) used a higher-resolution GFDL model with a simulated QBO and found good agreement with post–Mount Pinatubo temperature observations at 50 mb without including ozone changes, but that paper does not show results around 100 mb. Unfortunately, ozone changes after El Chichón versus Mount Pinatubo in the tropics are not well quantified, with some studies finding similar reductions in ozone after the two eruptions (Angell 1997b), while others seem to show larger changes for Mount Pinatubo (Fioletov et al. 2002). Water vapor changes are also not well known, especially for El Chichón and for the tropics. While the possible effects of such changes on the responses to Mount Pinatubo and El Chichón are therefore difficult to assess, ozone decreases after Mount Pinatubo could be a plausible explanation for the lack of warming at 100 mb in the observations (see Forster et al. 2007).

The Sato et al. (2001) aerosol optical depth data show most of the loading in the Southern Hemisphere for Mount Agung and in the Northern Hemisphere for El Chichón. This dataset is cited as the primary source for five of the six models we used. The sixth, PCM, has aerosol that is more evenly divided between the hemispheres for all three eruptions, with slightly more in the SH for both El Chichón and Mount Agung, and more in the NH for Mount Pinatubo. The PCM responses in the NHX for Pinatubo and Mount Agung are larger than those for most other models, and smaller for the SH for Mount Agung, perhaps for this reason. Although the differences in the forcings and the expected differences in response to the greater heat capacity in the ocean-dominated SH might be expected to give different hemispheric responses, the observed extratropical tropospheric responses are small in both hemispheres for El Chichón and Mount Pinatubo, and it is difficult to see a difference between the responses in the two regions for El Chichón. Mount Pinatubo observations do suggest more cooling in the NH, but this is not discernible in the model mean.

The mixed results regarding volcanic effects on trends in the models are consistent with the lack of systematic differences between the trends in models including volcanic forcings and those that do not include volcanoes, seen in Fig. 3 of Santer et al. (2005). Neither the iterative approach nor the method of dropping post-volcano years supports the hypothesis that volcanic cooling contributes significantly to the difference in trend between the surface and lower troposphere in the radiosonde data for 1979–99 in the tropics. The RATPAC and HADAT2 radiosonde data show trends at the surface

~0.1 K greater than those at 850–500 mb, while the models all show tropospheric trends similar to or greater than those at the surface. Our results indicate that volcanic cooling does not contribute more than ~0.03 K to this difference. This implies problems with the model simulations or the radiosonde data. As discussed in Lanzante and Free (2008) and work cited therein, the most likely explanation is the presence of inhomogeneities in these radiosonde datasets.

8. Conclusions

The vertical profile of temperature responses to the three major recent eruptions in six coupled climate models is generally similar to that in radiosonde data, with the following exceptions:

1) The modeled Mount Pinatubo signal shows distinctly more warming than observations between 150 and 70 mb in the tropics.
2) PCM and HadGEM show much more warming in the tropical stratosphere than do the other models or the observations.
3) The cooling from the El Chichón and Mount Pinatubo eruptions is greater in the tropical troposphere than at the surface, but this tropospheric amplification is much larger in the observations than in the model responses. While the observations show similar amplification for ENSO and the eruptions, the models respond with greater amplification for ENSO than for either Mount Pinatubo or El Chichón.
4) Upper-tropospheric tropical cooling tends to be smaller in the models than in the data, but these differences are mostly not statistically significant.
5) The largest differences between the observations and model responses occur for Mount Agung in the SHX troposphere, but these differences may be due to the relatively poor sampling in the SHX.
6) Differences among the model responses and between the modeled and observed effects are likely related to differences or errors in the volcanic or other forcings assumed, as well as in the observations, rather than deficiencies in the models themselves.

Estimates of the effects of the eruptions on trends are dependent on the method used and the choice of parameters, particularly the time scale of decay of the volcanic temperature effect. For the tropical tropospheric time series examined here, decay times of 20 months or less appear to fit better than longer ones. Using these shorter times gives estimated trend effects that are too small to account for the differences between modeled and observed tropical tropospheric temperature trends for the satellite period. For larger decay times, estimated effects are enough to bring observed mps trends in line with some model results for the upper tropical troposphere. The effect of volcanic eruptions on the differential temperature trends appears to be small for the least squares trends in the upper tropical troposphere, and is minimal for the lower troposphere.

Acknowledgments. We thank the modeling groups for making their simulations available for analysis, the Program for Climate Model Diagnosis and Intercomparison (PCMDI) for collecting and archiving the CMIP3 model output, and the WCRP's Working Group on Coupled Modelling (WGCM) for organizing the model data analysis activity. The WCRP CMIP3 multimodel dataset is supported by the Office of Science, U.S. Department of Energy. We also thank the reviewers for helpful comments. This research was supported in part by NOAA's Office of Global Programs.

APPENDIX

Iterative Method to Separate ENSO and Volcanic Signals (Based on Santer et al. 2001)

The method of Santer et al. (2001) involves an iterative procedure alternating the removal of ENSO and volcanic signals from a time series. Santer et al. (2001) used this method on global mean surface and MSU tropospheric temperatures. Here we apply it to regional mean temperatures at the surface and 12 atmospheric pressure levels from radiosonde data and model output. The method assumes a linear ramp-down of temperatures after the eruption, followed by an exponential decay of the volcanic cooling (Fig. 1). The rate of decay is specified, while the length for the linear ramp-down and the size of the maximum cooling are determined empirically for each time series by locating the minimum temperature within the 24 months after the eruption and determining the number of months between the eruption and that minimum. The volcanic signal constructed using this information is subtracted from the original time series and the ENSO signal is then calculated from the ENSO index using linear regression. After subtracting this ENSO signal from the original time series, the volcanic signal is estimated again and the procedure continues for a specified number of such iterations. To reduce the impact of short-term nonvolcanic variability, we smoothed the input time series using a 3- or 5-month running mean before finding the minimum temperature. We also smoothed the ENSO index with a 7-month running mean before performing the ENSO regression.

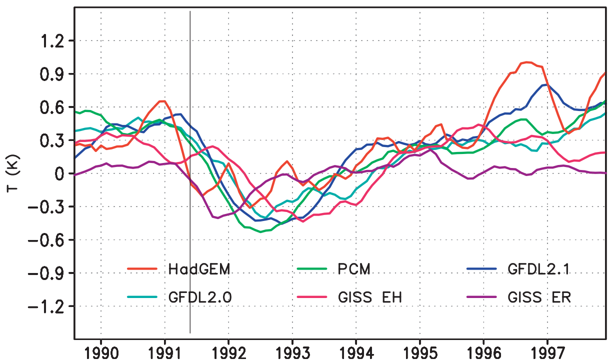

FIG. A1. Seven-month running means of ensemble means of model temperature time series (K) after removal of ENSO signals for 300 hPa in the tropics after the eruption of Mount Pinatubo in May 1991. Vertical line shows the time of the Mount Pinatubo eruption.

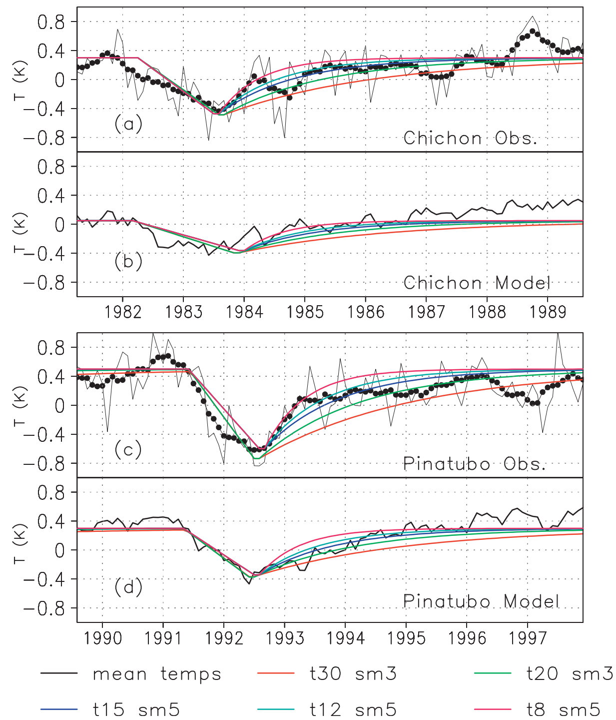

FIG. A2. Time series of temperature (K) at 300 mb in the tropics (black) with volcanic signals from iterative procedure using varying parameter settings (color), for (a) RATPAC observations and El Chichón, (b) the mean of six models for El Chichón, (c) RATPAC observations for Mount Pinatubo, and (d) the mean of six models for Mount Pinatubo. Model mean time series are detrended. RATPAC data are shown with (filled dots) and without (solid line) smoothing using a 7-month running mean. Decay parameters are 30 (t30), 20 (t20), 15 (t15), and 8 (t8) months, and smoothing values are 3-month (sm3) and 5-month (sm5) running means.

Santer et al. (2001) used cooling decay rates of 30–40 months. The postvolcanic temperature time series for the individual model ensemble means show varying shapes (Fig. A1), so the appropriate values of this parameter are not obvious and the actual shapes often do not follow the idealized expectation. The difference may be due at least in part to internal variability, or the true decay function may be more complex than the simple exponential decay assumed here (Boer et al. 2007). We tested decay values from 8 to 30 months and found that values of 20 months or less were generally closer to the RATPAC and model mean time series than were the larger values (Table A1), although larger values are more consistent with physical expectations (Santer et al. 2001). Figure A2 shows examples of these fits for RATPAC observations and six-model means at 300 mb in the tropics. The small apparent decay times may be the result of interference by internal variability; the difference between our results and those of Santer et al. (2001) could also reflect differences between the decay times in the tropics versus the globe. Unless otherwise indicated, we have used a decay constant of 20 months. The results are also sensitive to a lesser extent to the smoothing applied to the time series before estimation of the volcanic signal. Although the volcanic signals estimated with this method are only somewhat sensitive to the choice of decay parameter and the degree of smoothing used (Fig. A3), estimates of the effects of the eruptions on trends are very sensitive.

TABLE A1. Root-mean-square difference between model mean time series at 300 mb in the tropics and corresponding volcanic signal constructed using iterative procedure, for the 5 yr following the specified eruption, for varying values of the decay parameter (K).

	RMS difference (K)	
Decay parameter (months)	Mount Pinatubo	El Chichón
30	0.110	0.200
20	0.087	0.169
15	0.086	0.146
12	0.088	0.132
8	0.107	0.115

Santer et al. (2001) benefitted from their global and vertical (tropospheric) averaging, which suppressed much of the noise in the time series. Because we are working with individual pressure levels and regional rather than global means, our time series have considerable short-term variability that makes it difficult for an automated procedure to estimate the timing of the maximum volcanic effect. In the presence of random "noise," selecting the month with the minimum temperature after the volcano will tend to overestimate the effect of the volcano. This effect adds to the uncertainties inherent in any estimate of volcanic effects on temperatures.

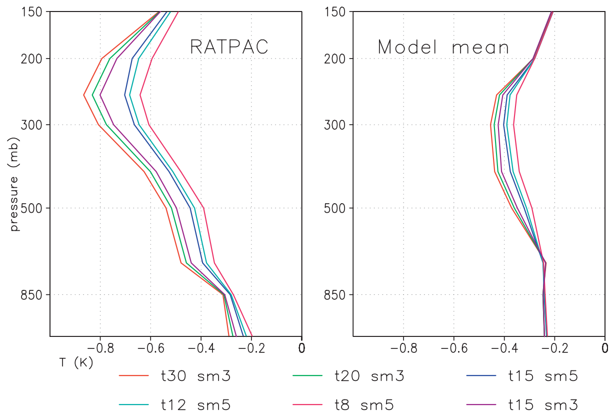

FIG. A3. Mount Pinatubo temperature response (K) for (left) RATPAC and (right) the mean of six models in the tropics averaged over the 2 yr after the eruption using the iterative method, for several choices of decay parameter and smoothing. Decay parameters are 30 (t30), 20 (t20), 15 (t15), and 8 (t8) months and smoothing values are 3- (sm3) and 5-month (sm5) running means.

The form of the volcanic signal used in Santer et al. (2001) cannot be applied directly to the stratosphere or the area near the tropopause that is influenced by the stratosphere because the chosen response shape was based on physical expectations that may not apply directly to stratospheric temperature changes and on examination of tropospheric mean temperature responses. In addition, applying this method in the tropical stratosphere would depend strongly on a near-complete removal of QBO effects, which would otherwise make it very difficult to determine the time of maximum volcanic effect.

REFERENCES

Ammann, C. M., G. A. Meehl, W. M. Washington, and C. S. Zender, 2003: A monthly and latitudinally varying volcanic forcing data set in simulations of 20th century climate. *Geophys. Res. Lett.,* **30,** 1657, doi:10.1029/2003GL016875.

Angell, J. K., 1988: Impact of El Niño on the delineation of tropospheric cooling due to volcanic eruptions. *J. Geophys. Res.,* **93** (D4), 3697–3704.

——, 1997a: Stratospheric warming due to Agung, El Chichón and Pinatubo taking into account the quasi-biennial oscillation. *J. Geophys. Res.,* **102,** 9479–9485.

——, 1997b: Estimated impact of Agung, El Chichón and Pinatubo volcanic eruptions on global and regional total ozone after adjustment for the QBO. *Geophys. Res. Lett.,* **24,** 647–650.

Boer, G. J., M. Stowasser, and K. Hamilton, 2007: Inferring climate sensitivity from volcanic events. *Climate Dyn.,* **28,** 481–502.

Delworth, T. L., and Coauthors, 2006: GFDL's CM2 global coupled climate models. Part I: Formulation and simulation characteristics. *J. Climate,* **19,** 643–674.

Deshler, T., A. Adriani, G. P. Gobbi, D. J. Hofmann, G. Di Donfrancesco, and B. J. Johnson, 1992: Volcanic aerosol and ozone depletion within the Antarctic polar vortex during the austral spring of 1991. *Geophys. Res. Lett.,* **19,** 1819–1822.

Fioletov, V. E., G. E. Bodeker, A. J. Miller, R. D. McPeters, and R. Stolarski, 2002: Global and zonal total ozone variations estimated from ground-based and satellite measurements: 1964–2000. *J. Geophys. Res.,* **107,** 4647, doi:10.1029/2001JD001350.

Forster, P. M., G. Bodeker, R. Schofield, S. Solomon, and D. Thompson, 2007: Effects of ozone cooling in the tropical lower stratosphere and upper troposphere. *Geophys. Res. Lett.,* **34,** L23813, doi:10.1029/2007GL031994.

Free, M., and J. K. Angell, 2002: Effect of volcanoes on the vertical temperature profile in radiosonde data. *J. Geophys. Res.,* **107,** 4101, doi:10.1029/2001JD001128.

——, D. J. Seidel, J. K. Angell, J. Lanzante, I. Durre, and T. C. Peterson, 2005: Radiosonde Atmospheric Temperature Products for Assessing Climate (RATPAC): A new data set of large-area anomaly time series. *J. Geophys. Res.,* **110,** D22101, doi:10.1029/2005JD006169.

Hansen, J., and Coauthors, 2007: Climate simulations for 1880-2003 with GISS modelE. *Climate Dyn.,* **29,** 661–696, doi:10.1007/s00382-007-0255-8.

Johns, T. C., and Coauthors, 2006: The new Hadley Centre Climate Model (HadGEM1): Evaluation of coupled simulations. *J. Climate,* **19,** 1327–1353.

Karl, T. R., S. J. Hassol, C. D. Miller, and W. L. Murray, Eds., 2006: Temperature trends in the lower atmosphere: Steps for understanding and reconciling differences. U.S. Climate Change Science Program and the Subcommittee on Global Change Research Rep., Synthesis and Assessment Product 1.1, 164 pp.

Lanzante, J. R., 1996: Resistant, robust and non-parametric techniques for the analysis of climate data: Theory and examples, including applications to historical radiosonde station data. *Int. J. Climatol.,* **16,** 1197–1226.

——, 2007: Diagnosis of radiosonde vertical temperature trend profiles: Comparing the influence of data homogenization versus model forcings. *J. Climate,* **20,** 5356–5364.

——, and M. Free, 2008: Comparison of radiosonde and GCM vertical temperature trend profiles in the troposphere and stratosphere: Effects of dataset choice and data homogenization. *J. Climate,* **21,** 5417–5435.

Lau, K.-M., C.-H. Ho, and I.-S. Kang, 1998: Anomalous atmospheric hydrologic processes associated with ENSO: Mechanisms of hydrologic cycle–radiation interaction. *J. Climate,* **11,** 800–815.

McCormick, M. P., L. W. Thomason, and C. R. Trepte, 1995: Atmospheric effects of the Mt Pinatubo eruption. *Nature,* **373,** 399–404.

Meehl, G. A., C. Covey, T. Delworth, M. Latif, B. McAvaney, J. F. B. Mitchell, R. J. Stouffer, and K. E. Taylor, 2007: The WCRP CMIP3 multi model dataset: A new era in climate change research. *Bull. Amer. Meteor. Soc.,* **88,** 1383–1394.

Parker, D. E., 1985: The influence of the Southern Oscillation and volcanic eruptions on temperature in the tropical troposphere. *Int. J. Climatol.,* **5,** 273–282.

——, H. Wilson, P. D. Jones, J. R. Christy, and C. K. Folland, 1996: The impact of Mount Pinatubo on world-wide temperatures. *Int. J. Climatol.,* **16,** 487–497.

Ramachandran, S., V. Ramaswamy, G. L. Stenchikov, and A. Robock, 2000: Radiative impact of the Mount Pinatubo volcanic eruption: Lower stratospheric response. *J. Geophys. Res.,* **105,** 24 409–24 429.

Randall, D., and Coauthors, 2007: Climate models and their evaluation. *Climate Change 2007: The Physical Basis*, S. Solomon et al., Eds., Cambridge University Press, 589–662.

Randel, W. J., F. Wu, and D. J. Gaffen, 2000: Interannual variability of the tropical tropopause derived from radiosonde data and NCEP reanalyses. *J. Geophys. Res.,* **105,** 15 509–15 524.

Robock, A., 2000: Volcanic eruptions and climate. *Rev. Geophys.,* **38,** 191–219.

Santer, B. D., and Coauthors, 2001: Accounting for the effects of volcanoes and ENSO in comparisons of modeled and observed temperature trends. *J. Geophys. Res.,* **106,** 28 033–28 060.

——, and Coauthors, 2005: Amplification of surface temperature trends and variability in the tropical atmosphere. *Science,* **309,** 1551–1556.

Sato, M., J. E. Hansen, M. P. McCormick, and J. B. Pollack, 1993: Stratospheric aerosol optical depths, 1850-1990. *J. Geophys. Res.,* **98,** 22 987–22 994.

Stenchikov, G., K. Hamilton, A. Robock, V. Ramaswamy, and M. D. Schwarzkopf, 2004: Arctic oscillation response to the 1991 Pinatubo eruption in the SKYHI general circulation model with a realistic quasi-biennial oscillation. *J. Geophys. Res.,* **109,** D03112, doi:10.1029/2003JD003699.

——, ——, R. J. Stouffer, A. Robock, V. Ramaswamy, B. Santer, and H.-F. Graf, 2006: Arctic Oscillation response to volcanic eruptions in the IPCC AR4 climate models. *J. Geophys. Res.,* **111,** D07107, doi:10.1029/2005JD006286.

Thorne, P. W., D. E. Parker, S. F. B. Tett, P. D. Jones, M. McCarthy, H. Coleman, and P. Brohan, 2005: Revisiting radiosonde upper-air temperatures from 1958 to 2002. *J. Geophys. Res.,* **110,** D18105, doi:10.1029/2004JD005753.

Washington, W. M., 2000: Parallel climate model (PCM) control and transient simulations. *Climate Dyn.,* **16,** 755–774.